



Cite this: *Photochem. Photobiol. Sci.*, 2016, **15**, 69

## Titania modification with a ruthenium(II) complex and gold nanoparticles for photocatalytic degradation of organic compounds

Shuaizhi Zheng,<sup>\*a,b</sup> Zhishun Wei,<sup>a</sup> Kenta Yoshiiri,<sup>a,c</sup> Markus Braumüller,<sup>b</sup> Bunsho Ohtani,<sup>a,c</sup> Sven Rau<sup>b</sup> and Ewa Kowalska<sup>\*a,c</sup>

Titania of fine anatase nanoparticles (ST01) was modified successively with two components, *i.e.*, a ruthenium(II) complex with phosphonic anchoring groups  $[\text{Ru}(\text{bpy})_2(4,4'-(\text{CH}_2\text{PO}_3\text{H}_2)_2\text{bpy})]^{2+}$  bpy = 2,2'-bipyridine ( $\text{Ru}^{\text{II}}\text{CP}$ ) and gold nanoparticles (Au). Various compositions of two titania modifiers were investigated, *i.e.*, Au, Au +  $\text{Ru}^{\text{II}}\text{CP}$ , Au + 0.5 $\text{Ru}^{\text{II}}\text{CP}$ ,  $\text{Ru}^{\text{II}}\text{CP}$ , 0.5 $\text{Ru}^{\text{II}}\text{CP}$  and 0.25 $\text{Ru}^{\text{II}}\text{CP}$ , where Au and  $\text{Ru}^{\text{II}}\text{CP}$  correspond to 0.81 mol% and 0.34 mol% (with respect to titania), respectively. In the case of hybrid photocatalysts, the sequence of modification (ruthenium(II) complex adsorption or gold deposition) was investigated to check its influence on the resultant properties and thus photocatalytic performance. Diffuse reflectance spectroscopy (DRS), X-ray photoelectron spectroscopy (XPS) and scanning transmission electron microscopy (STEM) were applied to characterize the structural properties of the prepared photocatalysts, which confirmed the successful introduction of modifiers of the ruthenium(II) complex and/or gold NPs. Different distributions of gold particle sizes and chemical compositions were obtained for the hybrid photocatalysts prepared with an opposite sequence. It was found that photocatalytic activities depended on the range of used irradiation (UV/vis or vis) and the kind of modifier in different ways. Gold NPs improved the photocatalytic activities, while  $\text{Ru}^{\text{II}}\text{CP}$  inhibited the reactions under UV/vis irradiation, *i.e.*, methanol dehydrogenation and acetic acid degradation. Oppositely,  $\text{Ru}^{\text{II}}\text{CP}$  greatly enhanced the photocatalytic activities for 2-propanol oxidation under visible light irradiation.

Received 21st September 2015,  
Accepted 12th November 2015

DOI: 10.1039/c5pp00345h

www.rsc.org/ppp

## Introduction

$\text{TiO}_2$  semiconductor materials have been widely used in the area of photocatalysis for decomposition of organic pollutants and clean fuel production,<sup>1,2</sup> due to their strong photocatalytic activity, high chemical stability, low cost and relatively non-toxic properties.<sup>3,4</sup> However, remaining challenges in  $\text{TiO}_2$ , such as rapid recombination of photogenerated electron/hole pairs, fast backward reactions (in the absence of efficient charge carrier scavengers) and inability to utilize the visible range of the solar spectrum, still need to be overcome to improve the photocatalytic efficiency and develop visible light-responsive materials.<sup>3</sup> Various modifications of titania, like noble metal loading, transition metal ion doping, nonmetal doping, sensitizer attachment, and composition with carbon nanomaterials have been extensively investigated in the past

few years.<sup>1–3,5–8</sup> Among these modifiers, gold nanoparticles (NPs)<sup>9,10</sup> and ruthenium(II) dyes<sup>11,12</sup> are excellent candidates to broaden the visible light performance of titania. Spherical Au NPs show surface plasmon absorption at around 500–700 nm (until the IR range for different shapes of gold nanostructures, such as nanorods, nanocages, nanoshells)<sup>13,14</sup> and ruthenium(II) complexes have the <sup>1</sup>MLCT (metal to ligand charge transfer) band centered at around 450 nm. An additional advantage of Au NPs in comparison with other noble metals (Ag and Cu) is their chemical stability, resistance to oxygen, and ability to serve as co-catalytic sites.<sup>15–17</sup> Gold NPs incorporated in DSSCs (dye-sensitized solar cells) were reported to enhance the solar conversion efficiency.<sup>18–20</sup> Meanwhile, ruthenium(II) complexes were also successfully applied towards visible light activation in DSSCs,<sup>21</sup> where the photoexcited electrons could be injected from ruthenium sensitizers to the conduction band of titania. The adaption of two modifiers to titania may lead to a synergistic effect, which might improve the photocatalytic performance.<sup>22–24</sup> Recently, we have investigated hybrid  $\text{TiO}_2$  photocatalysts composed of different kinds of titania (anatase, rutile and their mixture), plasmonic NPs (Au and Ag) and a  $[\text{Ru}(\text{bpy})_2(4,4'-(\text{PO}_3\text{H}_2)_2\text{bpy})]^{2+}$  sensitizer.<sup>25</sup> Different photocatalytic outcomes of enhancement or inhibition have been

<sup>a</sup>Institute for Catalysis, Hokkaido University, N21, W10, 001-0021 Sapporo, Japan.  
E-mail: xishuai423@hotmail.com, kowalska@cat.hokudai.ac.jp

<sup>b</sup>Institute of Inorganic Chemistry 1, Ulm University, Albert-Einstein-Allee 11, 89081 Ulm, Germany

<sup>c</sup>Graduate School of Environmental Science, Hokkaido University, N10, W5, 060-0810 Sapporo, Japan



observed for titania modified with two components, possibly due to the interaction between two modifiers. Therefore, in this paper, titania with different compositions of gold NPs and ruthenium(II) was applied to gain further insight into their roles during the photocatalytic reactions. Commercial titania (ST01) of anatase form and a high specific surface area (to provide the high capability of ruthenium(II) immobilization) was selected for this study.<sup>25</sup> Gold in the amount of 2 wt% to titania was applied based on our former results, which would provide an optimal light absorption when deposited on small anatase titania.<sup>26</sup> The ruthenium(II) complex of  $[\text{Ru}(\text{bpy})_2(4,4'-(\text{CH}_2\text{PO}_3\text{H}_2)_2\text{bpy})]^{2+}$  possessing an additional methylene unit between a phosphonate anchoring group and bpy was tested in the present study. The methylene spacer lengthens the electron transfer distance between the ruthenium(II) core and  $\text{TiO}_2$  surface,<sup>27,28</sup> therefore would potentially increase the lifetime of the excited states and change the electron transfer kinetics,<sup>29</sup> which are important factors governing the whole photocatalytic process. In addition, two deposition methods of inverse sequences (Au/Ru<sup>II</sup>CP or Ru<sup>II</sup>CP/Au) were adopted purposely to check whether it influences the resultant properties and thus the photocatalytic activities, as was suggested in the previous paper,<sup>25</sup> *i.e.*, it was proposed that ruthenium(II) could be adsorbed also on the metallic NPs instead of titania, especially in the case of positively charged silver NPs. On the other hand, it is also suspected that deposition of gold on ruthenium(II) modified titania should result in the formation of different sizes of gold NPs than in the case of direct gold deposition on a bare titania surface.

## Results and discussion

### Preparation of photocatalysts

**Gold deposition.** Gold was photodeposited on bare and ruthenium(II)-modified titania ST01 ( $\text{Au}/\text{TiO}_2 = 2\%$  w/w, 0.81%

$\text{mol mol}^{-1}$ ), and the obtained data of hydrogen evolution are shown in Fig. 1. During metal photodeposition on titania, the induction period (evident here as intersection with the  $x$ -axis in the left part of Fig. 1(a)) during which NPs of noble metals are formed, depends on the properties of metal and titania (*e.g.*, amount, kind and distribution of electron traps). In the case of gold deposition, usually less than fifteen minutes is sufficient to reduce all gold cations and form gold NPs, which is evident by a linear evolution of hydrogen at a constant rate.<sup>16,26</sup> Complete deposition of gold was confirmed in our previous studies for a wide range of gold concentrations from 0.05 to 10 wt% by atomic absorption spectroscopy.<sup>26</sup> Similarly, in the present study, gold photodeposition was very fast and after *ca.* 3 min of irradiation the linear evolution of hydrogen was noticed.

It was found that with the increase in the amount of Ru<sup>II</sup>CP on titania (0, 0.5, 1), the induction period of hydrogen generation became longer (2.3 min, 6.7 min and 13.7 min, respectively), as shown in Fig. 1(c). Similar results were obtained for deposition of gold on pre-modified titania with silver NPs, where silver hindered  $\text{Au}^{+3}$  reduction.<sup>16</sup> It is suggested that the charge on the titania surface from Ru<sup>II</sup>CP affects the following gold photodeposition, *i.e.*, ruthenium(II) complexes attached to titania with an overall negative charge, which contributed to the deprotonated phosphonate groups are repulsive to the  $\text{AuCl}_4^-$  ions. In addition, the steric hindrance caused by the ruthenium(II) complex could hinder the gold ions to reach the titania surface and thus their reduction by photogenerated electrons, as shown in the scheme presented in Fig. 1(b). Besides the two times longer induction time with the increase in the Ru<sup>II</sup>CP amount from 0.5 to 1, the rate of hydrogen generation also reduced by nearly half. It is expected that the adsorbed Ru<sup>II</sup>CP influences light harvesting by titania. The excited state properties of Ru<sup>II</sup>CP binding to titania showed the redox potential of  $-0.93$  V ( $\text{Ru}^{\text{III}}/\text{Ru}^{\text{II}*}$ ), which would be sufficient to inject electrons to the conduction band of titania

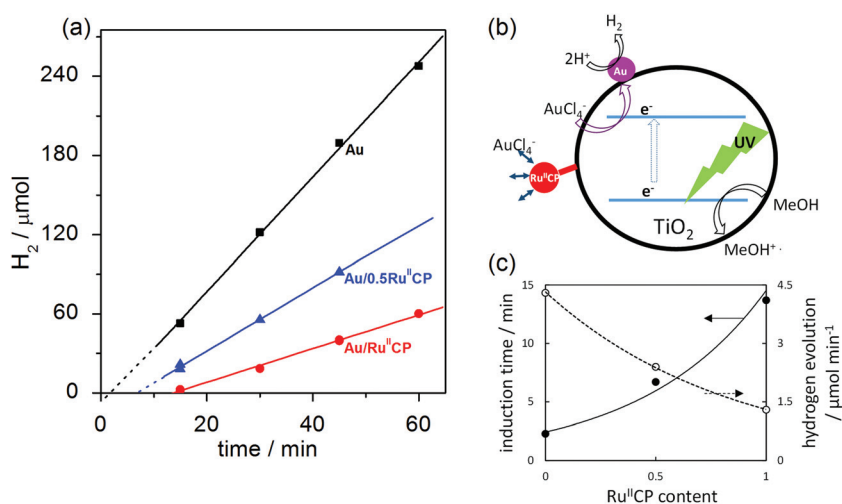


**Fig. 1** Methanol dehydrogenation during photodeposition of gold on bare and Ru<sup>II</sup>CP-modified titania (ST01): (a) hydrogen evolution with time, (b) proposed mechanism, (c) influence of Ru<sup>II</sup>CP amount on induction time and hydrogen evolution rate.



of  $-0.3$  V under similar conditions.<sup>30</sup> It is well known that the ruthenium complexes could inject electrons into the conduction band of titania under visible light irradiation. However, in the presence of UV light, the ruthenium complexes may also undergo ligand exchange with the solvent, decomposition or desorption, *etc.*, which might improve or inhibit the electron injection processes, *e.g.*, by adjusting the energy levels between the LUMO of the dye and the conduction band of titania.<sup>31</sup> Herein, two kinds of disturbances in titania photoabsorption properties could be considered, *i.e.*, (i) Ru<sup>II</sup>CP competes with titania for light absorption to excite the electrons from the bpy ligands, and/or (ii) the “inner filter effect” due to the dark color of ruthenium(II)-adsorbed TiO<sub>2</sub>, which can result in hindrance of light penetration through the titania suspension. It is expected that the latter one could be rejected since gold modified titania possessing the highest photocatalytic activity exhibited similar darkness (photoabsorption properties) as Au/Ru<sup>II</sup>CP (as shown in Fig. 3 and 4). Furthermore, the existence of induction time for Ru<sup>II</sup>CP modified titania suggests that the single modified titania with only Ru<sup>II</sup>CP should not possess meaningful activity (similar to bare titania samples) for hydrogen evolution.

As has been already mentioned, after the accomplishment of Au NP deposition, the hydrogen evolution processes started. Under UV/vis irradiation of titania, the electron is excited from the valence band (VB) to the conduction band (CB) leaving a hole in the VB. Herein, the Au NPs operate as the electron sinks, which trap and store the electrons from the CB, and then act as the reduction sites for hydrogen generation. For all the samples, the amount of gold was identical, *i.e.*, 2 wt% to titania. With the increase of Ru<sup>II</sup>CP content on titania, the rates of hydrogen evolution decreased ( $4.3 \mu\text{mol min}^{-1}$ ,  $2.4 \mu\text{mol min}^{-1}$  and  $1.3 \mu\text{mol min}^{-1}$ ). Such a phenomenon might reveal (in addition to the already mentioned compe-

titution for light absorption) that the second modifier (Ru<sup>II</sup>CP) inhibits the desirable electron transfer steps for hydrogen formation. Considering all the electron transfer steps, it is highly possible that the Au NPs might either interact with Ru<sup>II</sup>CP, or Ru<sup>II</sup>CP works also as an electron sink for the CB electrons, which has been already suggested by time-resolved microwave conductivity (TRMC) measurements.<sup>25</sup> The obtained data, *i.e.*, the induction periods and hydrogen evolution rates, during gold deposition, imply that Ru<sup>II</sup>CP inhibits the methanol dehydrogenation under UV/vis irradiation.

**Adsorption of ruthenium(II) complex.** For the immobilization of ruthenium(II) complexes on semiconductor materials, anchoring groups including phosphonate or carboxylate are very popular.<sup>32–37</sup> The anchoring group effects on the following titania sensitization are influenced by many factors, like solvent, co-existent electron donors, *etc.*, even the same sensitizer might show different behaviours in different environments.<sup>38</sup> The stability of surface binding is primarily related to the anchoring group. The phosphonate group instead of carboxylate has been frequently used to enhance the surface binding strength,<sup>39,40</sup> which also influences the overall photocatalytic activities. Our previous research also showed that the phosphonate group had more stable binding affinity to titania in an aqueous environment, where complete desorption occurred for ruthenium(II) with the carboxylate functional groups.<sup>25</sup> In this work, the complex with similar anchoring phosphonate groups to our previous work was kept to obtain a stable interfacial binding with titania, and an additional methylene spacer was introduced between the bipyridine motif and the phosphonate group, which lengthened the distance between the Ru<sup>II</sup>CP metal core and titania. Time dependent adsorption of the complex for the sample with the highest amount of Ru<sup>II</sup>CP was shown in Fig. 2(a). Adsorption of Ru<sup>II</sup>CP on titania ST01 was very fast similar to

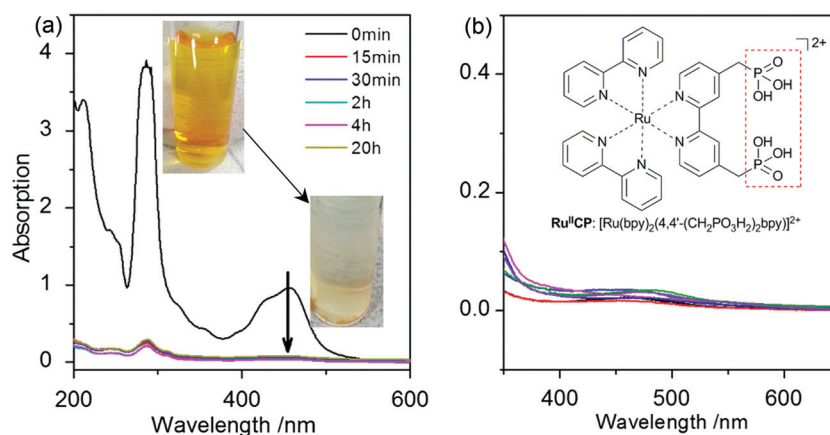


**Fig. 2** (a) Ru<sup>II</sup>CP adsorption behavior on bare titania ST01 in aqueous solution; the inset: photographs of bright orange color of Ru<sup>II</sup>CP aqueous solution used for adsorption, and colorless supernatant after Ru<sup>II</sup>CP mixing with titania; (b) absorption spectra of all photocatalysts after 90 min UV/vis irradiation during methanol dehydrogenation (colors of curves are respective to samples presented in Fig. 4); the inset: the structure of Ru<sup>II</sup>CP: [Ru(bpy)<sub>2</sub>(4,4'-(CH<sub>2</sub>PO<sub>3</sub>H<sub>2</sub>)<sub>2</sub>bpy)]<sup>2+</sup>. The absorption spectra were taken from the liquid phase of the suspension after removal of particles by centrifugation.



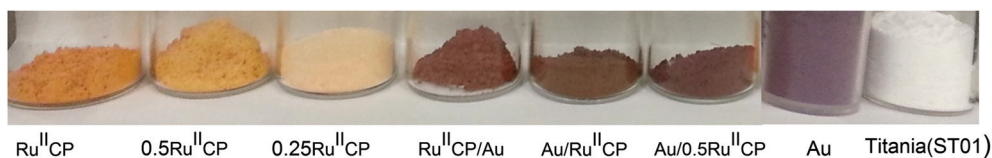


Fig. 3 Images of bare and modified titania (ST01) photocatalysts and their abbreviations.

$[\text{Ru}(\text{bpy})_2(4,4'-(\text{PO}_3\text{H}_2)_2\text{bpy})]^{2+}$  adsorption on the titanias of fine NPs (TIO10, P25, ST01, PC101, PC102),<sup>†</sup> where less than half an hour resulted in almost complete complex attachment.<sup>25</sup> At present, adsorption was even faster and the completion time was less than 5 min, which was reasonable, due to the small crystallite size and large specific surface area of titania ST01 causing efficient binding. The obtained data confirmed strong influence of the kind of titania on the adsorption behaviour.<sup>25</sup> The presence of pre-deposited gold and the used amount of  $\text{Ru}^{\text{II}}\text{CP}$  did not influence significantly the speed and the efficiency of complex adsorption. With the increasing concentration of  $\text{Ru}^{\text{II}}\text{CP}$  from 0.085 mol%, 0.17 mol% to 0.34 mol% (respectively to titania) on bare titania ST01, and 0.34 mol%  $\text{Ru}^{\text{II}}\text{CP}$  on gold pre-deposited titania, the adsorption processes are all very fast and efficient as discussed above.

The stability of attachment was investigated during long-lasting stirring of ruthenium(II) adsorbed titania in an aqueous suspension. It was found that even 24 h of stirring did not affect the  $\text{Ru}^{\text{II}}\text{CP}$  attachment. Moreover, even after 90 min strong UV/vis irradiation in MeOH/H<sub>2</sub>O (1 : 1), a negligible amount of ruthenium could be found in the liquid phase for all the adsorbed  $\text{Ru}^{\text{II}}\text{CP}$ -titania samples, which indicated its stable chemical binding to titania, as shown in Fig. 2(b). Thus, it was shown that the  $\text{Ru}^{\text{II}}\text{CP}$  adsorbed titania ST01 was robust under highly intensive energy of UV/vis irradiation conditions. It is important to address the stability, due to the requirement of applicable photocatalysts in industry.

### Characterization of photocatalysts

The adsorption of  $\text{Ru}^{\text{II}}\text{CP}$  on white titania led to the preparation of yellowish/orange powders of different color intensities depending on the amount of used  $\text{Ru}^{\text{II}}\text{CP}$ , as shown in Fig. 3. Single gold modified titania had violet color, typical for small, spherical gold NPs, due to localized surface plasmon

resonance (LSPR), while the samples with co-adsorbed  $\text{Ru}^{\text{II}}\text{CP}$  and Au NPs possessed purple brownish colors.

The absorption properties of the samples measured by diffuse reflectance spectroscopy (DRS) are shown in Fig. 4. The absorption of photocatalysts could be divided into three regions, *i.e.*, (1) band-gap absorption of titania in UV range, (2) MLCT of ruthenium(II) at *ca.* 420–480 nm, and (3) LSPR of gold NPs at *ca.* 520–620 nm. It must be pointed out that the DRS data showed not only photoabsorption, but also scattering. In this regard, a broader shoulder at longer wavelengths detected for titania modified with Au/ $\text{Ru}^{\text{II}}\text{CP}$  than with  $\text{Ru}^{\text{II}}\text{CP}/\text{Au}$  and Au indicates the presence of larger gold NPs, mainly due to enhanced scattering. It was reported that intense scattering, detected as a broad shoulder at longer wavelengths than LSPR, was observed with an increase in the gold NP size from 10 nm to 50 nm.<sup>41</sup>

In this regard, it is expected that the pre-adsorbed  $\text{Ru}^{\text{II}}\text{CP}$  disturbed the Au deposition and formation of fine gold NPs, and thus probably aggregates of gold NPs were formed on  $\text{Ru}^{\text{II}}\text{CP}$  adsorbed titania. To check this hypothesis, STEM observations were performed for titania modified with Au/ $\text{Ru}^{\text{II}}\text{CP}$ ,  $\text{Ru}^{\text{II}}\text{CP}/\text{Au}$  and Au, and the exemplary STEM images with histograms of gold NP sizes are shown in Fig. 5.

The comparison of gold NP sizes is shown in Fig. 4(b). The obtained data confirmed that the presence of ruthenium(II) highly influenced the aggregation of gold NPs. It was found that the mean size of gold NPs was in the range of 11–15 nm for titania modified with Au and  $\text{Ru}^{\text{II}}\text{CP}/\text{Au}$ , while in the case of Au/ $\text{Ru}^{\text{II}}\text{CP}$  much larger NPs were formed of 26–30 nm. In addition, it must be pointed out that in the case of gold deposition on the pre-modified titania with  $\text{Ru}^{\text{II}}\text{CP}$ , gold NPs possessed much broader distribution of their sizes (from 5 to 85 nm) and shapes (even nanorods and nanotriangles). Surprisingly, adsorption of  $\text{Ru}^{\text{II}}\text{CP}$  on gold modified titania caused a slight change in the distribution of gold sizes and a larger amount of small NPs of 6–10 nm were detected than in the case of single modified titania with Au, probably due to reshaping. Gold reshaping could be influenced by thermal treatment, a gold immobilized material,<sup>42</sup> the presence of a surfactant, an inorganic salt,<sup>43</sup> *etc.* It is possible that the introduction of a second modifier could result in the change of the titania environment, like surface charge. The distribution of gold NP sizes correlates well with photoabsorption properties for all samples containing gold, *i.e.*, the larger the gold NPs are, the broader is the shoulder of the DRS spectrum at longer wavelengths.

Three STEM modes were used for the observation of the morphology of samples, *i.e.*, secondary electron (SE), Z-con-

<sup>†</sup> Sample abbreviations<sup>44</sup>

Name	Supplier	Composition	Crystalline size/nm	Particle size/ $\mu\text{m}$	BET/ $\text{m}^2\text{g}^{-1}$
ST01	Ishihara	A	8	5.86	298
PC101	TK	A	8	1.6	301
PC102	TK	A	12	1.44	157
P25	Degussa	A/R	28	0.94	59
TIO10	CSJ	A	15	2.5	100

A: anatase. R: rutile. TK: Titan Kogyo (PC series). CSJ: Catalysis Society of Japan.



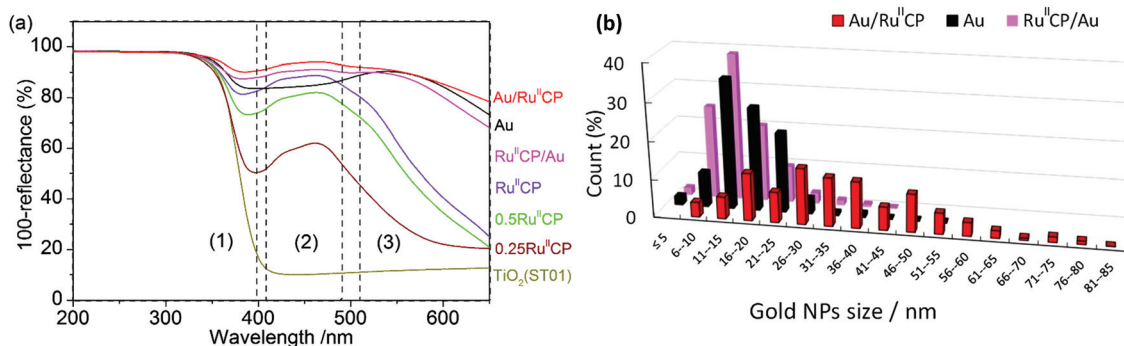


Fig. 4 (a) DRS spectra of bare and modified titania (ST01) photocatalysts with marked ranges of photoabsorptions for: (1) titania band-gap, (2) MLCT of Ru<sup>II</sup>CP and (3) LSPR of Au NPs; (b) distribution of gold NP sizes based on STEM measurements (shown in Fig. 5).

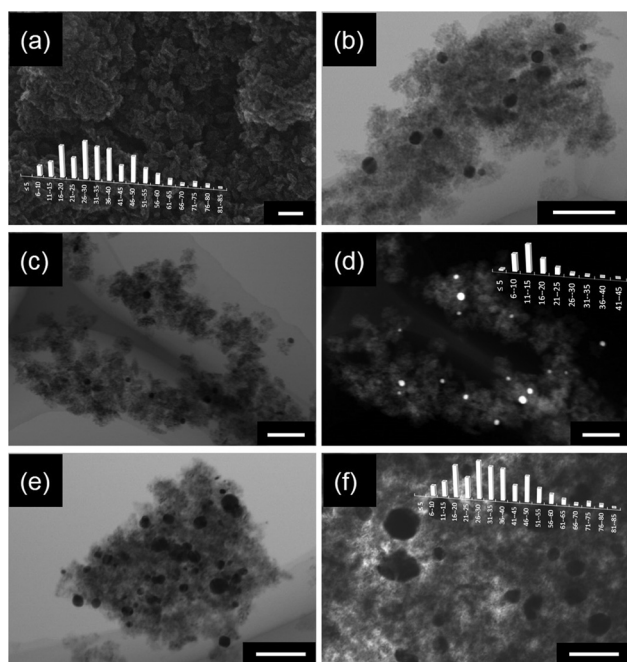


Fig. 5 STEM images with respective histograms of gold NP sizes for titania (ST01) samples modified with Au (a and b), Ru<sup>II</sup>CP/Au (c and d) and Au/Ru<sup>II</sup>CP (e and f); scale bar: 100 nm.

trast (ZC) and bright-field (TE) modes. Titania ST01 possesses very fine NPs of anatase of less than 10 nm (8 nm from XRD measurements),<sup>44</sup> and thus very fine anatase nano-crystallites in the form of aggregates are clearly observed in all the images shown in Fig. 5. It is difficult to distinguish gold from titania by simple SE mode, as shown in Fig. 5(a). Therefore for calculation of gold size distribution, TE and ZC modes were used, in which gold NPs are observed as darker and lighter spots, respectively, as clearly presented in Fig. 5(c) and (d), which show the same view of the Ru<sup>II</sup>CP/Au sample. It is easily observable even without histograms that much larger gold NPs were formed in the case of gold deposition on Ru<sup>II</sup>CP-modified titania (Fig. 5e and f).

To characterize the composition of photocatalysts and to check the possibility of self-co-adsorption of modifiers, *i.e.*, Ru<sup>II</sup>CP on Au or Au on Ru<sup>II</sup>CP, X-ray photoelectron spectroscopy (XPS) analysis was performed, and the obtained data are shown in Fig. 6 and Table 1. The presence of gold was confirmed in all titania samples containing gold, *i.e.*, Au, Ru<sup>II</sup>CP/Au and Au/Ru<sup>II</sup>CP, and its amount slightly exceeded that which was used for photodeposition (0.81 mol%) reaching 1.23, 0.88 and 1.08 mol%, respectively. Though, the differences between gold amounts are small, the lowest amount of gold (0.88 mol%) in the Ru<sup>II</sup>CP/Au sample suggests that the ruthenium(II) complex could partly adsorb on the gold surface.

Similar to our previous findings<sup>25</sup> gold was mainly in the zero-charged form in all the tested samples (91–100%). A small content (<3%) of positively charged gold (Au<sup>σ+</sup>) in the Au/TiO<sub>2</sub> sample could result from Au–O–Ti linkages formed at the metal–support interface as has already been proposed for Au–TiO<sub>2</sub> aerogels.<sup>45</sup> This slight positive charge of gold could support the hypothesis of partial ruthenium(II) complex adsorption on the gold surface instead of titania. Similar data were reported for preferential CO adsorption on Au<sup>σ+</sup> of Au/TiO<sub>2</sub>(P25) photocatalyst.<sup>45</sup> It should be mentioned that various surface charges of gold NPs deposited on titania were reported, *i.e.*, mainly zero, but also negatively (as the result of the transfer of electron density from the oxide support to Au NP)<sup>46</sup> and positively charged.<sup>45</sup> Our previous data for gold deposited on the other titania (P25) photocatalyst containing two crystalline (anatase and rutile) and amorphous titania forms (*ca.* 78, 14 and 8%, respectively)<sup>47</sup> showed the existence of gold mainly in zero charged form (89%) with small amounts of both negative (9%) and positive (2%) states.<sup>25</sup> Therefore, it is suggested that the support properties significantly influence the resultant properties of deposited metallic NPs. While, the lower amount of gold in Au than in Au/Ru<sup>II</sup>CP modified titania could be caused by smaller particle sizes of gold in this sample, where more gold surface was covered by fine titania resulting in a decrease in the detected amount of gold.

The atomic ratio of oxygen to titania significantly exceeded 2.0 for bare titania (6.9) indicating titania surface enrichment with hydroxyl groups. This was also confirmed by deconvolu-



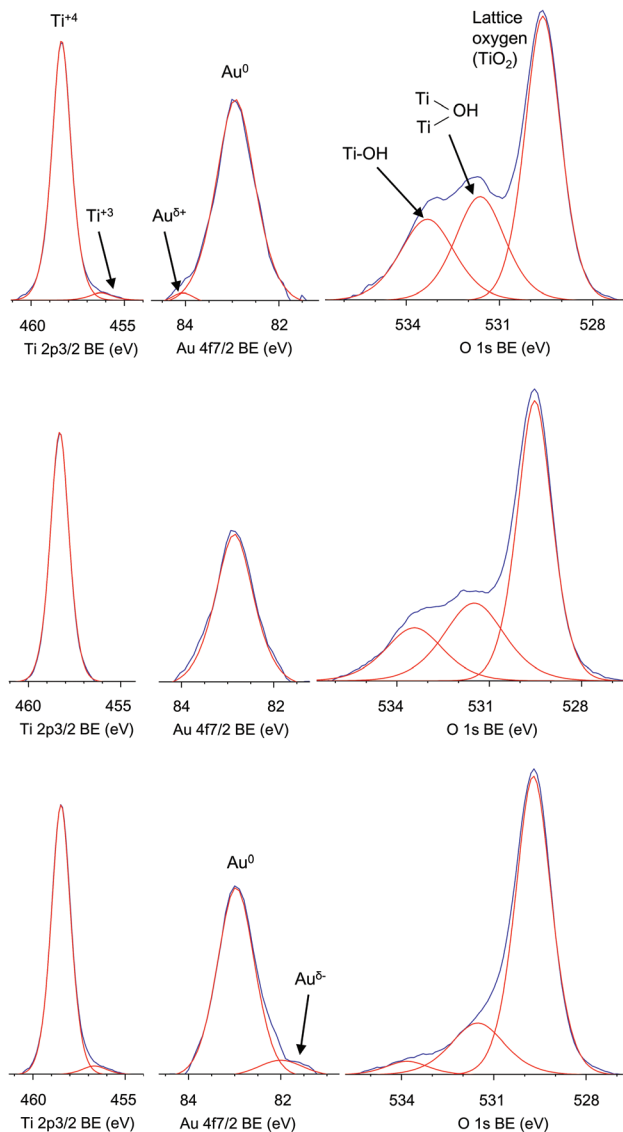


**Fig. 6** XPS data of titania (STO1) modified with Au (top), Ru<sup>II</sup>CP/Au (middle) and Au/Ru<sup>II</sup>CP (bottom) for titanium 2p<sub>3/2</sub> (left), gold 4f<sub>7/2</sub> (center) and oxygen 1s (right).

**Table 1** Chemical composition of bare and modified samples based on XPS analysis

Sample	Ti (mol%)	O (mol%)	O : Ti	C (mol%)	Au (mol%)	Au : Ti (mol%)
Titania (STO1)	4.04	27.81	6.9	68.14	—	—
Ru <sup>II</sup> CP	7.44	30.12	4.1	62.44	—	—
Au	12.99	35.14	2.7	51.71	0.16	1.23
Ru <sup>II</sup> CP/Au	14.74	38.95	2.6	46.18	0.13	0.88
Au/Ru <sup>II</sup> CP	24.93	45.85	1.8	28.95	0.27	1.08

tion of an oxygen peak, which shows an existence of oxygen mainly in the form of free (44%) and bounded (31%) hydroxyl groups (Table 1). The modification of titania resulted in a decrease in the atomic ratio of oxygen to titania to 4.1, 2.7, 2.6

and 1.8 for Ru<sup>II</sup>CP, Au, Ru<sup>II</sup>CP/Au and Au/Ru<sup>II</sup>CP, respectively, which indicates the substitution of surface oxygen by modifiers and/or the decrease in the adsorbed water on the titania surface. After deconvolution of titanium, oxygen and gold peaks, it was found that titanium existed mainly in the Ti<sup>4+</sup> form and gold in the Au<sup>0</sup> form. In the case of hybrid photocatalysts, change in the deposition sequence resulted in the preparation of samples slightly different in their properties, *i.e.*, the Ru<sup>II</sup>CP/Au sample consisted of only Ti<sup>4+</sup> and Au<sup>0</sup>, while the Au/Ru<sup>II</sup>CP sample possessed also a small amount of Ti<sup>3+</sup> (*ca.* 4%), Au<sup>δ-</sup> (*ca.* 9%), and a much smaller amount of oxygen on the surface (especially in the -OH form).

### Photocatalytic dehydrogenation of methanol under UV/vis irradiation

As has already been discussed in the preparation of photocatalysts, during gold deposition on different supports (with and without ruthenium(II)), hydrogen was generated from methanol suspensions of titania samples modified with Au/Ru<sup>II</sup>CP, Au/0.5Ru<sup>II</sup>CP and Au. To gain a systematical overview, all the samples were irradiated with UV/vis to compare their photocatalytic activities for methanol dehydrogenation, and the results are shown in Fig. 7. The rates of hydrogen evolution for Au/Ru<sup>II</sup>CP, Au/0.5Ru<sup>II</sup>CP and Au, retained the same trend with the aforementioned results (Fig. 1(a)), but the values changed due to the different conditions used for photoactivity testing than during sample preparations (*ca.* 5 and 20 times lower amounts of methanol and photocatalysts, respectively).

Bare titania was practically inactive for alcohol dehydrogenation, attributed to fast recombination of photogenerated charge carriers, and the low driving force for the H<sup>+</sup> reduction reaction, resulting in slow H<sup>+</sup> reduction kinetics.<sup>48</sup> Hydrogenation usually occurs on the co-catalyst site, which collects the photogenerated electrons.<sup>49–51</sup> Herein, the presence of Au enhances the photocatalytic activity of titania by *ca.* 13 times, working as a co-catalyst. However, the samples with Ru<sup>II</sup>CP and 0.5Ru<sup>II</sup>CP inhibit the photocatalytic activity of bare titania STO1. These results are very surprising since our previous report for a similar ruthenium(II) complex showed an enhancement of photocatalytic activity for four different titania samples after adsorption of [Ru(bpy)<sub>2</sub>(4,4'-(PO<sub>3</sub>H<sub>2</sub>)<sub>2</sub>bpy)]<sup>2+</sup>,<sup>25</sup> which suggested that hydrogen evolution occurred on the Ru site according to the enhancement outcome. The inhibition, observed in the present study, might be caused by different structures of the attached ruthenium(II) complex. It is highly possible that TiO<sub>2</sub>(e<sup>-</sup>)-Ru(III) is formed, and the presence of the -CH<sub>2</sub>- linker slows down the electron transfer, which means that the electrons are faster transferred to titania than are captured by protons. It was observed that during photoirradiation, the suspension with only Ru<sup>II</sup>CP modified photocatalyst turned greenish, which could be owing to Ru(III) formation. Also, under UV/vis irradiation, it could undergo other reactions as we mentioned in the gold deposition section. Therefore, the Ru<sup>II</sup>CP did not result in improvement of the photocatalytic activity in this case. The presence of both modifiers increased the photocatalytic activity when compared



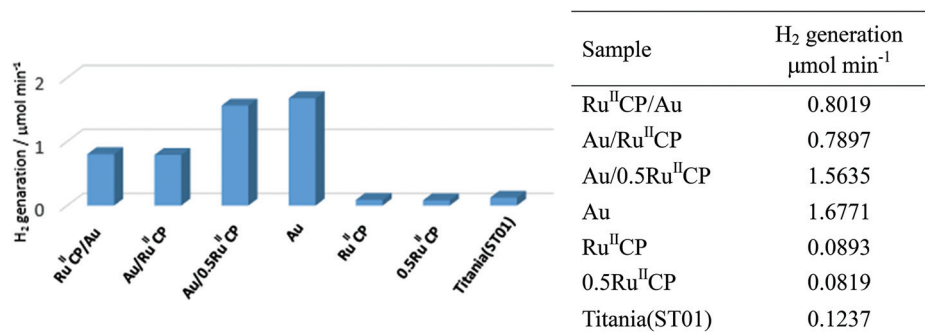


Fig. 7 Photocatalytic activity for methanol dehydrogenation under UV/vis irradiation.

to bare titania, but decreased it when compared to the gold modified sample. Moreover, reduced amount of Ru<sup>II</sup>CP resulted in an increase of photocatalytic activity, *i.e.*, titania modified with Au/0.5Ru<sup>II</sup>CP showed *ca.* two times higher photocatalytic activity than Au/Ru<sup>II</sup>CP. These results are also quite different than those reported for [Ru(bpy)<sub>2</sub>(4,4'-(PO<sub>3</sub>H<sub>2</sub>)<sub>2</sub>bpy)]<sup>2+</sup> for which even a synergetic effect was observed between Au and ruthenium(II) modifiers for a titania photocatalyst of fine NPs (TIO10).<sup>25</sup> Thus, it is suggested that the methylene group between the ruthenium coordinated bipyridine and phosphonate groups strongly hindered the electron transfer between titania and ruthenium. To clarify the mechanism of hydrogen evolution the action spectra experiments are presently under study.

Notably, Au/Ru<sup>II</sup>CP and Ru<sup>II</sup>CP/Au showed nearly the same rate of dehydrogenation with about six-fold enhancement to bare titania, which means that the preparation sequences do not affect the photocatalytic activities under UV/vis irradiation conditions. Moreover, it could suggest that even if ruthenium(II) attached partly to the metallic surface (Au) instead of the titania surface, as was suggested in our previous paper<sup>25</sup> and confirmed here by the XPS data, this attachment is not crucial for the overall activity.

Therefore, the conclusion that gold improves, but ruthenium(II) inhibits the photocatalytic activity could be drawn in the case of fine anatase titania and the [Ru(bpy)<sub>2</sub>(4,4'

(CH<sub>2</sub>PO<sub>3</sub>H<sub>2</sub>)<sub>2</sub>bpy)]<sup>2+</sup> complex for methanol dehydrogenation under UV/vis irradiation.

### Photocatalytic decomposition of acetic acid under UV/vis irradiation

Photocatalysts were also tested in another reaction system, *i.e.*, under aerobic conditions for acetic acid degradation under UV/vis light irradiation, and the results are shown in Fig. 8.

It was confirmed that single modification of titania with gold resulted in an increase in photocatalytic activity, *ca.* 1.3 times. The introduction of ruthenium(II) inhibited the photocatalytic reactions and the photocatalytic rates for the samples with only ruthenium(II) modifier were slightly lower. Furthermore, for the co-modified titania, a lower amount of Ru<sup>II</sup>CP resulted in a higher level of photocatalytic activity, *i.e.*, titania modified with Au/0.5Ru<sup>II</sup>CP was more active than Au/Ru<sup>II</sup>CP. The change of deposition sequences (Au and Ru<sup>II</sup>CP) did not affect the photocatalytic activity confirming that both modifiers mainly deposited individually and there were no direct interactions between them. These results were consistent with those for methanol dehydrogenation and are discussed above. Au primarily serves as an electron trap which leads to the higher activity of acetic acid degradation. While for Ru<sup>II</sup>CP, its adsorption on titania may reduce the surface bond hydroxyl groups as also proved by the XPS data in Table 2, which under photoreaction would produce surface bond hydroxyl radicals

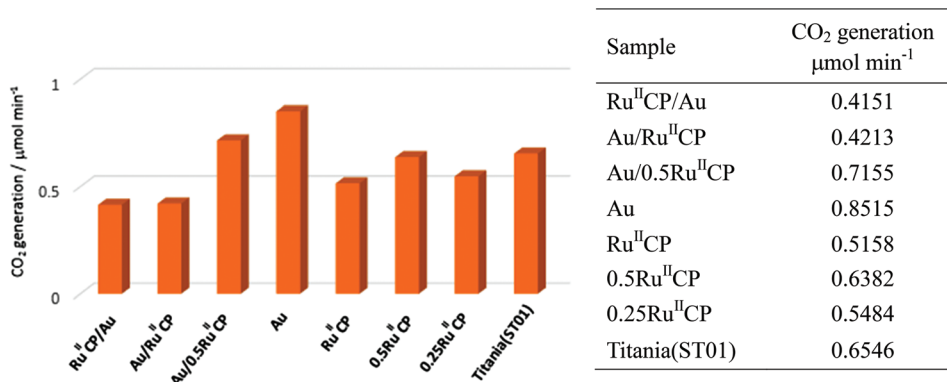


Fig. 8 Photocatalytic activity for acetic acid degradation under UV/vis irradiation.



**Table 2** Oxidation states of titanium, oxygen and gold based on XPS analysis

Sample	Ti 2p (%)		O 1s (%)			Au 4f (%)		
	Ti <sup>+4</sup>	Ti <sup>+3</sup>	–OH	–(OH) <sub>2</sub>	TiO <sub>2</sub>	Au <sup>δ+</sup>	Au <sup>0</sup>	Au <sup>δ–</sup>
Titania(ST01)	100	—	44.1	31.3	24.7	—	—	—
Ru <sup>II</sup> CP	98.5	1.5	25.9	36.3	37.8	—	—	—
Au	96.8	3.2	22.3	26.1	51.7	2.9	97.1	—
Ru <sup>II</sup> CP/Au	100	—	26.8	17.4	55.8	—	100	—
Au/Ru <sup>II</sup> CP	96.1	3.9	4.1	19.7	76.2	—	90.9	9.1

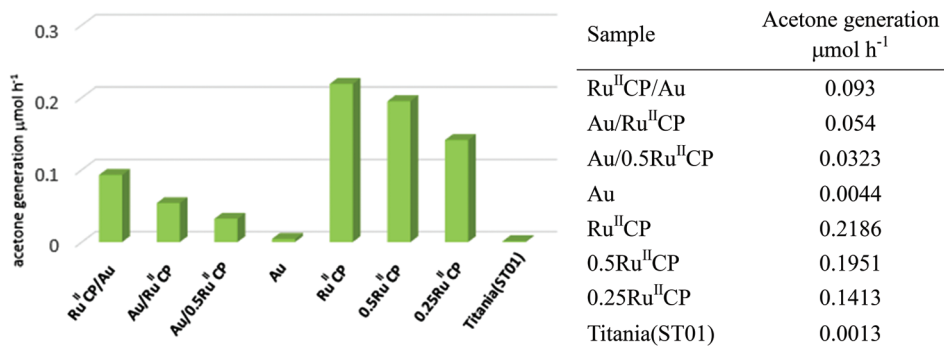
(the reaction between photogenerated holes and surface bond hydroxyl), as was proposed by W. Choi for phosphonate modified titania.<sup>22</sup> Hence, mobile hydroxyl radicals (the production of holes with adsorbed water), which are strong oxidant species and may break the ruthenium by oxidizing its –CH<sub>2</sub>– spacer would be preferred in the presence of Ru<sup>II</sup>CP.<sup>28</sup> However, for the [Ru(bpy)<sub>2</sub>(4,4'-(PO<sub>3</sub>H<sub>2</sub>)<sub>2</sub>bpy)]<sup>2+</sup> complex contradictory results were obtained, *i.e.*, (i) enhancement of activity after titania modification with ruthenium(II) for all four anatase titania samples, and only decrease of activity for rutile titania, (ii) enhancement of activity for all hybrid photocatalysts containing Au and ruthenium(II) in comparison with single modification with ruthenium(II) or Au (decrease only for the rutile sample). Considering this, it is proposed that the previously investigated ruthenium phosphonate complex was not decomposed under similar conditions, due to the lack of the methylene group, where enhancement of photocatalytic behaviour was observed. Surely, the kind of titania should also be considered, since it influences the electron injection efficiency as well.<sup>52</sup> These data strongly suggest that a slight change in the structure of the ruthenium(II) complex caused a strong influence on the resultant properties and thus on the photocatalytic activities.

### Photocatalytic oxidation of 2-propanol under visible light irradiation

Under visible light irradiation, among all the photocatalysts, titania singly modified with ruthenium(II) displayed the highest photocatalytic activity for oxidation of 2-propanol, *i.e.*,

about 150-fold enhancement was achieved in comparison with bare titania, and the results are shown in Fig. 9. It should be pointed out that such high enhancement partly resulted from the experimental conditions in this study, *i.e.*, irradiation with wavelengths longer than 450 nm (Y48 filter) to ensure the elimination of photocatalytic activity of bare titania. In addition, it was found that the reaction rates of samples possessing different contents of ruthenium (Ru<sup>II</sup>CP, 0.5Ru<sup>II</sup>CP, 0.25Ru<sup>II</sup>CP, 0Ru<sup>II</sup>CP and also hybrid samples: Au/Ru<sup>II</sup>CP and Au/0.5Ru<sup>II</sup>CP) decreased with a decreasing amount of attached Ru<sup>II</sup>CP, which indicates that the number of the injected electrons to titania is in a direct correlation with the photosensitizers. It is proposed that upon visible light irradiation, the ruthenium(II) injects electrons into the CB of titania, from where they are taken up by oxygen to form the reactive oxygen species (ROS), and finally ROS oxidize 2-propanol. At the same time, other reactions like back electron transfer processes and side reactions of the decomposition products also proceed. Moreover, oxidation of the methylene spacer could also occur in the presence of ROS, therefore the degradation of the attached ruthenium(II) or its detachment could occur.<sup>28</sup> To clarify the mechanism, transient spectroscopy is recommended as the next step to gain further details on the ET kinetics.

To compare two slightly different ruthenium(II) complexes used in present and previous reports, *i.e.*, ([Ru(bpy)<sub>2</sub>(4,4'-(CH<sub>2</sub>PO<sub>3</sub>H<sub>2</sub>)<sub>2</sub>bpy)]<sup>2+</sup> and [Ru(bpy)<sub>2</sub>(4,4'-(PO<sub>3</sub>H<sub>2</sub>)<sub>2</sub>bpy)]<sup>2+</sup>, respectively), the photocatalytic activity of the most active samples was tested. It was found that two times higher photocatalytic activity was achieved for titania TIO10 (anatase of fine NPs, similar to

**Fig. 9** Photocatalytic activity for oxidation of 2-propanol under visible light irradiation.

ST01) modified with  $[\text{Ru}(\text{bpy})_2(4,4'-(\text{PO}_3\text{H}_2)_2\text{bpy})]^{2+}$  than for the most active sample in the present study composed of  $[\text{Ru}(\text{bpy})_2(4,4'-(\text{CH}_2\text{PO}_3\text{H}_2)_2\text{bpy})]^{2+}$ . It is suggested that the additional methylene group hinders the electron transfer from ruthenium to the CB of titania or could be oxidized as discussed above.

It is important to mention that Au modified titania (ST01) selected for the present study possessed one of the least photocatalytic activities among other gold modified titanias, *e.g.*, almost eight times lower than that of rutile titania with gold NPs of various sizes and shapes (Au/TiO<sub>2</sub>(TiO5)).<sup>44</sup> This sample was selected to allow a high specific surface area for efficient adsorption of both modifiers (ruthenium(II) and Au) individually on the titania surface. Additionally, ruthenium(II)-modified titania of a high specific surface area exhibited much higher activity than that of a small specific surface area, *i.e.*, 40-times increase in photocatalytic activity was noticed with 33-fold increase in the specific surface area.<sup>25</sup> However, it must be pointed out that different behaviours and interactions between gold and Ru<sup>II</sup>CP could be expected for more active gold modified titania of broader LSPR.

For the dual modified titania, since both gold and ruthenium(II) should activate titania under visible light, enhancement of photocatalytic activity was expected. However, different behavior was observed, upon ruthenium(II) introduction to gold modified titania, the photocatalytic activity enhanced, but after introduction of gold to ruthenium(II) modified titania, a decrease in photocatalytic activity was noticed by about 4 and 6 times for Ru<sup>II</sup>CP and 0.5Ru<sup>II</sup>CP samples, respectively. Such a drop effect was also observed previously for other anatase titania samples modified with  $[\text{Ru}(\text{bpy})_2(4,4'-(\text{PO}_3\text{H}_2)_2\text{bpy})]^{2+}$ .<sup>25</sup> Therein, we proposed that the gold NPs serve as an electron sink to trap the electrons (similarly as under UV-activation of titania), which are transferred to the CB of TiO<sub>2</sub> from ruthenium(II) sensitizers, therefore hindering the electron scavenging by oxygen. Under current conditions, it is difficult to clarify the function of oxygen, which could lead to different mechanisms.<sup>53</sup> The experiments under anaerobic conditions are currently under investigation.

These results strengthened the importance of ruthenium(II) for oxidation of 2-propanol under visible light irradiation, and showed that the presence of gold NPs inhibited the photocatalytic activities of ruthenium(II) modified titania. Interestingly, the samples with co-adsorbed ruthenium(II) and gold NPs, which only differed in the deposition sequence, exhibited very different activities, *i.e.*, Ru<sup>II</sup>CP/Au was more active than Au/Ru<sup>II</sup>CP, in contrast to the results obtained under UV/vis irradiation of methanol (anaerobic) and acetic acid (aerobic) where both the samples exhibited the same activity (Fig. 7 and 8). It is supposed that during the preparation of the latter, the repulsive ruthenium complex induced gold aggregation and thus larger Au NPs were formed (which was confirmed by the DRS data and STEM also). It must be pointed out that the size of plasmonic NPs is important in the visible photocatalytic processes, and generally the larger the size of gold NPs is, the higher is photocatalytic activity under visible light

irradiation.<sup>51,54</sup> However, in the present system, it seems that the function of gold is different, *i.e.*, an electron trap instead of titania activation, and the larger NPs should exhibit better electron storage properties than the smaller NPs.

It is thought that the present findings could also be helpful for mechanism clarification for plasmonic photocatalysts composed of a wide band-gap semiconductor (usually titania) and plasmonic NPs. Two main mechanisms are suggested under visible light irradiation, *i.e.*, energy<sup>55</sup> and electron<sup>10</sup> transfers from excited plasmonic NPs to titania. The decrease in activity by co-modification with the ruthenium(II) complex and gold indicates that the electron transfer is more probable than the energy transfer mechanism in the present case. To gain better insight into the mechanism further research studies like dynamic study of charge excitation and recombination are necessary.

## Experimental

### Materials

Titania ST01 from Ishihara (anatase, specific surface area of *ca.* 300 m<sup>2</sup> g<sup>-1</sup>) was used as received. Ru<sup>II</sup>CP:  $[\text{Ru}(\text{bpy})_2(4,4'-(\text{CH}_2\text{PO}_3\text{H}_2)_2\text{bpy})]^{2+}$  was synthesized according to an analogue complex in the literature.<sup>56</sup> Water for solution preparation and sample washing was from the Milli-Q purification system. Hydrogen tetrachloroaurate(III) tetrahydrate (HAuCl<sub>4</sub>·4H<sub>2</sub>O) (Nacalai Tesque and Wako Pure Chemical Industry) was used as received for gold deposition. Methanol, acetic acid, 2-propanol, and acetone (Wako Pure Chemical Industry) were used without further purification.

### Preparation of photocatalysts

Ruthenium(II) was adsorbed on bare and pre-modified titania with Au (2 wt%) in an aqueous suspension by 3 min sonication, followed by 24-hour stirring in the dark. The mixture was centrifuged, washed three times with water, dried overnight at 100 °C, and ground in an agate mortar. Different amounts of Ru<sup>II</sup>CP corresponding to 0.34 mol% (Ru<sup>II</sup>CP), 0.17 mol% (0.5Ru<sup>II</sup>CP) and 0.085 mol% (0.25Ru<sup>II</sup>CP) to titania, were applied. For the sample of the highest amount of ruthenium(II), the time dependent adsorption (with UV/vis spectroscopy) was performed to ensure that 24 hours is sufficient for the completion of ruthenium(II) attachment.

2 wt% of gold, which corresponds to 0.81 mol% to titania, was photodeposited on the surface of bare and pre-modified titania with Ru<sup>II</sup>CP by the photodeposition method from 50 vol% aqueous methanol. The details of photodeposition were shown in our previous reports.<sup>16,26</sup>

### Characterization of photocatalysts

Samples were characterized by diffuse reflectance spectroscopy (DRS), X-ray photoelectron spectroscopy (XPS) and scanning transmission electron microscopy (STEM). DRS measurements were performed on a JASCO V-670 equipped with a PIN-757



integrating sphere. Barium sulfate and bare titania (ST01) were used as references during measurements.

The surface composition of samples and oxidation states of elements were measured by XPS on a JEOL JPC-9010MC (MgK $\alpha$  X-ray). 50 scans were carried out for each sample and the average data were taken for determination of titanium, oxygen and carbon. While 500 scans were performed for characterization of gold.

The morphology of samples was observed by STEM on a HITACHI HD2000 at 200-kV accelerating voltage and 30  $\mu$ A emission current. The droplet of titania suspension (in ethanol) was deposited on carbon-covered copper microgrid, which was dried overnight under vacuum at room temperature. STEM images were acquired as secondary electron (SE), Z-contrast (ZC) and bright-field (TE) modes. For calculation of distribution of gold NP sizes, 449, 460 and 361 NPs of gold were measured for titania samples modified with Au, Ru<sup>II</sup>CP/Au and Au/Ru<sup>II</sup>CP, respectively.

### Tests of photocatalytic activity

The photocatalytic activities were examined under UV/vis irradiation (400 W, high-pressure mercury lamp) for methanol dehydrogenation (50 vol% methanol under argon) and acetic acid oxidation (5 vol% acetic acid in air). Visible light photocatalytic activity was examined for 2-propanol oxidation (5 vol% 2-propanol in air) at wavelengths longer than 450 nm (300 W xenon lamp, IR filter, quartz mirror, Y48 cut-off filter). Characterization of set-ups used for irradiation is described in detail in a previous publication.<sup>44</sup>

## Conclusions

Ruthenium(II) dye and gold NPs were immobilized on the surface of anatase titania with fine NPs. The photocatalysts were stable since the complex did not desorb even after long-lasting UV/vis irradiation. It was found that under UV/vis irradiation the photocatalysts modified with gold exhibited the highest photocatalytic activities for both tested systems, *i.e.*, anaerobic methanol dehydrogenation and aerobic acetic acid degradation, and introduction of Ru<sup>II</sup>CP decreased the photocatalytic activities. On the contrary, under visible irradiation, gold hindered the photocatalytic activity of ruthenium(II).

The DRS, XPS and STEM characterization suggested that the pre-adsorbed ruthenium(II) complex on the titania surface affected the gold deposition, causing aggregation and a broader distribution of gold NP sizes. Also, the introduction of ruthenium(II) induced the change of gold NP sizes, which needs further exploration. This might be utilized to control the metal particle sizes, which can be useful for catalytic (dark) and photocatalytic reactions (it is known that gold size is a key-factor of many reactions).

It was found that the sequence of deposition (ruthenium(II) complex and gold NPs) did not significantly influence the photocatalytic activity under UV/vis irradiation. However, under visible light irradiation formation of slightly larger gold

NPs resulted in stronger inhibition of ruthenium(II) activity. It is proposed that larger gold NPs store electrons from the CB of titania (sensitized by ruthenium(II)) hindering their transfer to oxygen.

In addition, it must be pointed out that a small change in the ruthenium(II) complex structure results in a complete change of photocatalytic performance. It is proposed that direct bonding of the bipyridine motif with phosphonate groups allows a better electronic contact and electron transfer between titania and the ruthenium(II) complex. Besides, the presence of the methylene group would also risk the self-oxidation reaction causing dye degradation. In order to achieve the desirable synergetic effects when designing the hybrid photocatalysts, durable ruthenium(II) dyes under photocatalytic conditions with stable attachment properties to allow efficient electron transfer with titania and/or co-deposited metal particles should be considered. The new elongated phosphonate bipyridines, which utilize phenylene and triazole moieties instead of a flexible linker, seem interesting, since they provide  $\pi$ -conjugated systems between ruthenium(II) and titania,<sup>29</sup> and also may avoid the oxidation reaction on alkylene linkers.

Detailed investigation on the charge transfer process under specified irradiation ranges (*e.g.*, action spectrum analysis) is still required to clarify the mechanism. It is also recommended to examine other titania supports since titania properties should also influence the mechanism pathways, *e.g.*, by electron storage, recombination of charge carriers and/or preferential self-co-adsorption of ruthenium(II) dyes and gold.

## Acknowledgements

This research was funded by a grant from the CONCERT-Japan Joint Call.

## References

- 1 S. M. Gupta and M. Tripathi, *Chin. Sci. Bull.*, 2011, **56**, 1639–1657.
- 2 M. Pelaez, N. T. Nolan, S. C. Pillai, M. K. Seery, P. Falaras, A. G. Kontos, P. S. M. Dunlop, J. W. J. Hamilton, J. A. Byrne, K. O'Shea, M. H. Entezari and D. D. Dionysiou, *Appl. Catal., B*, 2012, **125**, 331–349.
- 3 M. Ni, M. K. H. Leung, D. Y. C. Leung and K. Sumathy, *Renewable Sustainable Energy Rev.*, 2007, **11**, 401–425.
- 4 P. Pichat, *J. Adv. Oxid. Technol.*, 2010, **13**, 238–246.
- 5 H. Park, Y. Park, W. Kim and W. Choi, *J. Photochem. Photobiol., C*, 2013, **15**, 1–20.
- 6 P. Chen, L. Wang, P. Wang, A. Kostka, M. Wark, M. Muhler and R. Beranek, *Catalysts*, 2015, **5**, 270–285.
- 7 W. Macyk, G. Burgeth and H. Kisch, *Photochem. Photobiol. Sci.*, 2003, **2**, 322–328.
- 8 D. Mitoraj and H. Kisch, *Angew. Chem., Int. Ed.*, 2008, **47**, 9975–9978.



- 9 C. Wang and D. Astruc, *Chem. Soc. Rev.*, 2014, **43**, 7188–7216.
- 10 Y. Tian and T. Tatsuma, *J. Am. Chem. Soc.*, 2005, **127**, 7632–7637.
- 11 K. Hirano, E. Suzuki, A. Ishikawa, T. Moroi, H. Shiroishi and M. Kaneko, *J. Photochem. Photobiol., A*, 2000, **136**, 157–161.
- 12 M. Grätzel, *J. Photochem. Photobiol., C*, 2003, **4**, 145–153.
- 13 E. Taboada, I. Angurell and J. Llorca, *J. Catal.*, 2014, **309**, 460–467.
- 14 M. Hu, J. Chen, Z.-Y. Li, L. Au, G. V. Hartland, X. Li, M. Marquez and Y. Xia, *Chem. Soc. Rev.*, 2006, **35**, 1084–1094.
- 15 M. Serra, J. Albero and H. García, *ChemPhysChem*, 2015, **16**, 1842–1845.
- 16 E. Kowalska, M. Janczarek, L. Rosa, S. Juodkazis and B. Ohtani, *Catal. Today*, 2014, **230**, 131–137.
- 17 P. A. DeSario, J. J. Pietron, D. E. DeVantier, T. H. Brintlinger, R. M. Stroud and D. R. Rolison, *Nanoscale*, 2013, **5**, 8073–8083.
- 18 T.-H. Meen, J.-K. Tsai, S.-M. Chao, Y.-C. Lin, T.-C. Wu, T.-Y. Chang, L.-W. Ji, W. Water, W.-R. Chen, I.-T. Tang and C.-J. Huang, *Nanoscale Res. Lett.*, 2013, **8**, 450.
- 19 T. Bora, H. H. Kyaw, S. Sarkar, S. K. Pal and J. Dutta, *Beilstein J. Nanotechnol.*, 2011, **2**, 681–690.
- 20 H. Choi, W. T. Chen and P. V. Kamat, *ACS Nano*, 2012, **6**, 4418–4427.
- 21 B. O'Regan and M. Grätzel, *Nature*, 1991, **353**, 737–740.
- 22 J. Kim and W. Choi, *Appl. Catal., B*, 2011, **106**, 39–45.
- 23 J. Kim, J. Lee and W. Choi, *Chem. Commun.*, 2008, 756–758.
- 24 J. Kim and W. Choi, *Energy Environ. Sci.*, 2010, **3**, 1042–1045.
- 25 E. Kowalska, K. Yoshiiri, Z. Wei, S. Zheng, E. Kastl, H. Remita, B. Ohtani and S. Rau, *Appl. Catal., B*, 2015, **178**, 133–143.
- 26 E. Kowalska, S. Rau and B. Ohtani, *J. Nanotechnol.*, 2012, **2012**, 1–11.
- 27 D. L. Ashford, W. Song, J. J. Concepcion, C. R. K. Glasson, M. K. Brennaman, M. R. Norris, Z. Fang, J. L. Templeton and T. J. Meyer, *J. Am. Chem. Soc.*, 2012, **134**, 19189–19198.
- 28 K. Hanson, M. K. Brennaman, A. Ito, H. Luo, W. Song, K. A. Parker, R. Ghosh, M. R. Norris, C. R. K. Glasson, J. J. Concepcion, R. Lopez and T. J. Meyer, *J. Phys. Chem. C*, 2012, **116**, 14837–14847.
- 29 M. Braumüller, D. Sorsche, M. Wunderlin and S. Rau, *Eur. J. Org. Chem.*, 2015, **27**, 5987–5994.
- 30 K. Hanson, M. K. Brennaman, A. Ito, H. Luo, W. Song, K. A. Parker, R. Ghosh, M. R. Norris, C. R. K. Glasson, J. J. Concepcion, R. Lopez and T. J. Meyer, *J. Phys. Chem. C*, 2012, **116**, 14837–14847.
- 31 K. Nonomura, Y. Xu, T. Marinado, D. P. Hagberg, R. Zhang, G. Boschloo, L. Sun and A. Hagfeldt, *Int. J. Photoenergy*, 2009, **2009**, 1–9.
- 32 N. A. Anderson and T. Lian, *Annu. Rev. Phys. Chem.*, 2005, **56**, 491–519.
- 33 E. Galoppini, *Coord. Chem. Rev.*, 2004, **248**, 1283–1297.
- 34 A. S. Polo, M. K. Itokazu and N. Y. Murakami Iha, *Coord. Chem. Rev.*, 2004, **248**, 1343–1361.
- 35 H. Zabri, I. Gillaizeau, C. A. Bignozzi, S. Caramori, M.-F. Charlot, J. Cano-Boquera and F. Odobel, *Inorg. Chem.*, 2003, **42**, 6655–6666.
- 36 I. Gillaizeau-Gauthier, F. Odobel, M. Alebbi, R. Argazzi, E. Costa, C. A. Bignozzi, P. Qu and G. J. Meyer, *Inorg. Chem.*, 2001, **40**, 6073–6079.
- 37 E. Bae, W. Choi, J. Park, H. S. Shin, S. Bin Kim and J. S. Lee, *J. Phys. Chem. B*, 2004, **108**, 14093–14101.
- 38 E. Bae and W. Choi, *J. Phys. Chem. B*, 2006, **110**, 14792–14799.
- 39 H. Park, E. Bae, J.-J. Lee, J. Park and W. Choi, *J. Phys. Chem. B*, 2006, **110**, 8740–8749.
- 40 K. Hanson, M. K. Brennaman, H. Luo, C. R. K. Glasson, J. J. Concepcion, W. Song and T. J. Meyer, *Appl. Mater. Interfaces*, 2012, **4**, 1462–1469.
- 41 Y. Xia and N. J. Halas, *MRS Bull.*, 2005, **30**, 338–348.
- 42 H. Pan, S. Low, N. Weerasuriya and Y.-S. Shon, *ACS Appl. Mater. Interfaces*, 2015, **7**, 3406–3413.
- 43 M. Iqbal and G. Tae, *J. Nanosci. Nanotechnol.*, 2006, **6**, 3355–3359.
- 44 E. Kowalska, O. O. P. Mahaney, R. Abe and B. Ohtani, *Phys. Chem. Chem. Phys.*, 2010, **12**, 2344–2355.
- 45 D. A. Panayotov, P. A. DeSario, J. J. Pietron, T. H. Brintlinger, L. C. Szymczak, D. R. Rolison and J. R. Morris, *J. Phys. Chem. C*, 2013, **117**, 15035–15049.
- 46 W.-T. Chen, A. Chan, Z. H. N. Al-Azri, A. G. Dosado, M. A. Nadeem, D. Sun-Waterhouse, H. Idriss and G. I. N. Waterhouse, *J. Catal.*, 2015, **329**, 499–513.
- 47 A. Markowska-Szczupak, K. Wang, P. Rokicka, M. Endo, Z. Wei, B. Ohtani, A. W. Morawski and E. Kowalska, *J. Photochem. Photobiol., B*, 2015, **151**, 54–62.
- 48 A. Reynal, F. Lakadamyali, M. A. Gross, E. Reisner and J. R. Durrant, *Energy Environ. Sci.*, 2013, **6**, 3291–3300.
- 49 A. J. Bard, *J. Photochem.*, 1979, **10**, 59–75.
- 50 A. Dawson and P. V. Kamat, *J. Phys. Chem. B*, 2001, **105**, 960–966.
- 51 E. Kowalska, R. Abe and B. Ohtani, *Chem. Commun.*, 2009, 241–243.
- 52 R. Katoh, A. Huijser, K. Hara, T. J. Savenije and L. D. A. Siebbeles, *J. Phys. Chem. C*, 2007, **111**, 10741–10746.
- 53 D. Pei and J. Luan, *Int. J. Photoenergy*, 2012, **2012**, 262831.
- 54 L. Du, A. Furube, K. Hara, R. Katoh and M. Tachiya, *Thin Solid Films*, 2009, **518**, 861–864.
- 55 D. B. Ingram, P. Christopher, J. L. Bauer and S. Linic, *ACS Catal.*, 2011, **1**, 1441–1447.
- 56 M. Braumüller, M. Schulz, D. Sorsche, M. Pfeffer, M. Schaub, J. Popp, B.-W. Park, A. Hagfeldt, B. Dietzek and S. Rau, *Dalton Trans.*, 2015, **44**, 5577–5586.

